CMST (Early View) 1–11 (2023) DOI:10.12921/cmst.2023.0000026

Isomorph Scaling of Hard Sphere and Lennard-Jones Fluids

D.M. Heyes[1*], **S. Pieprzyk**[2], **A.C. Brańka**[2]

[1] *Royal Holloway, University of London*
Department of Physics
Egham, Surrey TW20 0EX, United Kingdom
E-mail: david.heyes@rhul.ac.uk

[2] *Polish Academy of Sciences*
Institute of Molecular Physics
M. Smoluchowskiego 17, 60-179 Poznań, Poland

Received: 8 November 2023; in final form: 12 November 2023; accepted: 13 November 2023

Abstract: The transport coefficients of model monatomic fluids are explored within the context of isomorph theory. An extension of our previous study in this field to the thermal conductivity of Lennard-Jones (LJ) fluids is reported here. The relationship to and comparisons with the behavior of the LJ system and those of hard spheres (HS), which form perfect isomorphs at all densities are made. The HS and LJ transport coefficients obtained by MD simulations when scaled by so-called macroscopic ('isomorph') units, and the density is scaled by the freezing density, form curves which are extremely similar, and in near quantitative agreement apart from close to freezing in most cases. It is shown that to a large extent the excellent 'isomorph' scaling of the transport coefficients exhibited by the LJ system, even at low densities, can be traced back to the dominance of the repulsive part of this potential for these dynamical quantities, which can reasonably accurately be accounted for by the scaling behavior of hard spheres. Numerical support for this conclusion using molecular dynamics data for the HS and LJ model fluids is presented.

Key words: isomorphs, transport coefficients, monatomic fluids, molecular dynamics simulation

I. Introduction

The transport coefficients (TC) of small molecule ($e.g.$, argon and nitrogen) gases and liquids are of practical importance and of considerable interest from a theoretical perspective. The main TC of typical interest are the shear viscosity, η_s, the self-diffusion coefficient, D and the thermal conductivity, λ. The viscosity and thermal conductivity are useful as input parameters in continuum level simulations of various hydrodynamic flows, for example, in the Navier-Stokes modelling of shock-waves [1, 2]. It is important to know the self-diffusion coefficient for modelling at a continuum level chemical processes in solution, for example, heavy metal ion transfer in rivers [3].

This work addresses some fundamental issues of relevance to these objectives by being concerned with the scaling properties of transport coefficient of real fluids using the Lennard-Jones (LJ) potential as a convenient model test system.

For about 100 years the hard sphere (HS) fluid has been used as a reference for the physical and thermodynamic properties of real molecule systems whose effective pair interactions are continuous but steeply repulsive at short range. The HS potential is an extreme limiting case of such a short range repulsive potential. The HS system has found widespread use in forming the basis of, for example, perturbation theories of the thermodynamic properties of liquids [4], and also via Enskog's theory, of their transport coefficients [5–7].

The starting point for formulating a theory of the small molecule transport coefficients is the Boltzmann equation, which predicts the evolution of an assembly of point parti-

cles described in a probabilistic way assuming that a series of uncorrelated binary collisions of the particles takes place. Enskog extended this approximate treatment to include excluded volume effects ($i.e.$, the fact that two molecules cannot occupy the same space if they overlap to any significant extent) but retaining the random or uncorrelated collision approximation [5–7].

Molecular Dynamics (MD) computer simulation has over the last *ca.* 60 years shown that Enskog's equation is a remarkably accurate representation of the HS fluid system, except close to the freezing density for some of the TC, both in terms of the magnitude of the TC as a function of number density, and in the near exponential decay of the time correlation functions at short times ($i.e.$, less than the mean time between the collisions of a given particle). The actual HS system as modelled by MD becomes more viscous than the LJ fluid close to the freezing point than predicted by Enskog theory (ET) because of many particle cooperative dynamical effects between the particles which are not accounted for in ET.

An additional feature of the HS system, which is often not specifically commented on, is that the predicted TC ('X') (and other physical and thermodynamic properties) have a relatively trivial temperature dependence. At a given number density, ρ, the $\eta_{\rm s}, \lambda$ and D increase with increasing temperature, T, ($i.e.$, $X \propto \sqrt{T}$) [8]. Increasing the temperature means the same temporal distribution of assembly states but appearing at a faster rate. Therefore, for example, $\eta_{\rm s}/\sqrt{T}$ is a constant at all temperatures with a fixed density. In more recent terminology, this feature is referred to as the system exhibiting 'isomorphic' behavior, which means that the thermodynamic and TC (ρ, T) phase diagram is in practice one dimensional. This applies to phases with the same symmetry, and is also applicable therefore to solids which maintain the same crystal structure over the given density and temperature range, although the discussion in this work will implicitly be concerned with fluids.

This simple and conceptually useful scaling behavior extends to that of the (also widely studied) model inverse power (IP) potential fluid system (a list of the acronyms used in this work is given in Tab. 1). The IP pair potential is $\phi(r) = \epsilon(\sigma/r)^n$, where ϵ and σ are the charactistic energy of interaction and diameter of the two particles, respectively, r is the separation between the centers of the two particles, and $n > 3$ is the 'stiffness' exponent. In the $n \to \infty$ limit, the IP potential approaches the HS case and the IP static properties converge to those of the HS, although there are some differences between certain HS and IP dynamical properties such as the time correlation functions which arise from the discontinuous nature of the HS potential, while the IP potential is continuous no matter how large n is [9–11]. The IP phase diagram isomorph is defined by a series of lines in the density-temperature plane where $\rho^{n/3}/T$ is a constant, as was proved from statistical mechanics by Hoover *et al.* [12] to apply to the static and dynamical properties.

The HS and IP systems form perfect isomorphs, and in the HS case this is particularly simple, as each isomorph is a vertical line at a given HS number density on the density-temperature plane, on the abscissa-ordinate axes respectively.

Consider two IP or HS state points (denoted by the subscripts, '0' and '1') of a model system of particles at densities, ρ_0 and ρ_1 and temperatures, T_0 and T_1. The term 'isomorph' which means literally, 'constant form or structure' has the useful consequence that when the coordinates of the particles of state point 0 are scaled by the factor $[\rho_0/\rho_1]^{1/3}$ then if, $T_1 = T_0[\rho_1/\rho_0]^{1/3}$ these two state points are thermodynamically and dynamically identical after ensemble or time averaging. This is in the sense that the physical and dynamical properties are the same when scaled in so-called isomorph or 'macroscopic' units (MU) which makes each quantity dimensionless. For example, for the average potential energy of the system, U, this means that $U_0/k_{\rm B}T_0 = = U_1/k_{\rm B}T_1$, where $k_{\rm B}$ is Boltzmann's constant, which simplifies considerably the description of the system. A quantity, Y, expressed in MU is denoted by $\tilde{Y}$, and hence the above equality can be rewritten concisely as, $\tilde{U}_0 = \tilde{U}_1$ in MU. The transport coefficients investigated here are defined in MU in the next section.

For the LJ model system the IP $\rho^{n/3}/T$ relationship applies in the arbitrarily high temperature limit (where $n = 12$ in this case), which is called the 'high temperature limit' in this work.

The Lennard-Jones pair potential is defined as follow, $\phi(r) = 4\epsilon[(\sigma/r)^{12} - (\sigma/r)^6]$, where again ϵ and σ set the energy and lengthscales, respectively. It might be expected that because of the different density scaling of the repulsive ($i.e.$, $\sim (\sigma/r)^{12}$) and attractive, ($i.e.$, $\sim -(\sigma/r)^6$) parts of the total potential energy that the LJ system should not form isomorphs. However, over the last two decades it has been shown that the LJ (and other model potential) systems can exhibit isomorphic behavior *to a good approximation*. While this can be ascribed in part to the increasing dominance of the repulsive part of the potential in the high temperature limit, this cannot be the entire explanation. This is because these isomorphs can continue down to temperatures in the liquid region which terminate on the liquid side of the vapor-liquid binodal or on the freezing line. This is a region where the attractive interactions become increasingly important in a (perhaps) non-additive way in determining the physical properties, and cannot be neglected. The LJ isomorph (ρ, T) line increasingly deviates from the IP isomorph line as the temperature decreases from the high temperature limit (it shifts to higher density at a given temperature [13]). In the high temperature limit the LJ system and its properties converge to those of the $n = 12$ IP system (note that the IP ϵ is replaced by 4ϵ in this comparison).

While all the properties of an IP and HS system exhibit isomorph or macroscopic scaling, this is not the case for the LJ system. For example, while the radial distribution function shows an excellent degree of collapse when r is replaced by $r\rho^{1/3}$, and $\eta_{\rm s}, \lambda$ and D in MU also collapse to the same value along an isomorph when expressed in macroscopic units, the pressure and the bulk viscosity, $\eta_{\rm B}$, in MU do not. This can be simply explained for some properties but is not so obvious why it is for others. For example, for the pressure a model system potential may be the sum of terms whose potential energy (for example) components scale differently with density. This may in part explain why

the bulk viscosity does not scale with MU, as the pressure of the system is involved in its definition. The bulk viscosity and the other three transport coefficients are often computed by MD using the Green-Kubo time correlation function approach [14]. The bulk viscosity can also be calculated by a non-equilibrium molecular dynamics method invented by Hoover *et al.* [15, 16]. The fundamental reason for these often 'sharp' differences still requires further investigation.

The excess entropy, $s_{\rm ex}$, is defined as the difference between the total entropy of the system and its ideal gas value if it were at the same temperature and density [17]. An isomorph for the LJ and other non-IP systems has to satisfy two criteria. It has to be a line of constant excess entropy, $s_{\rm ex}$, which has been termed a 'configurational adiabat'. In addition the property of interest has to show the scaling collapse when expressed in MU (when this happens, the system is said to be a 'strongly correlated' for that property). It is the case that all the state points of a fluid fall on a configurational adiabat but not all configurational adiabats are isomorphs for a given property (if any). An isomorph has to be a configurational adiabat but a configurational adiabat does not also have to be an isomorph for a property of interest.

Previous MD and theoretical treatments of the transport coefficients of the hard sphere and Lennard-Jones (and other molecular systems) have commented on their similarity. One of the puzzling features is the good 'isomorphic' unit collapse of the data at low densities, where the LJ system does not exhibit isomorphs in the thermodynamic quantities. This has led to the introduction of the term 'isodyne' for such an occurrence, $i.e.$, where the transport coefficients collapse to a single value on an isodyne (ρ, T) line, when expressed in macroscopic units, but the static properties do not exhibit comparable lines in that density region. The reason why isodynes appear to be more prevalent than isomorphs is worthy of further consideration, and one of the main aspects of this work.

There are a variety of ways in which isomorphs can be mapped out in practice for a model system using molecular simulation. One way is to increment the density and temperature in small steps using a thermodynamic formula which is consistent with a constant excess entropy [18, 19]. Another procedure, called the Direct Isomorph Check (DIC) method, uses the requirement that along an isomorph the potential energies of any two configurations at two state points connected by uniform density scaling of the particle coordinates have to be strongly correlated [18, 20, 21]. Another more recent method is a variant of the DIC method, which employs the forces on the individual molecules of a single particle assembly configuration [22, 23]. In the latter two methods a 'virtual' isomorph state is generated by scaling the coordinates of the particles and the MD box sidelength to a new proposed density, and then determining the isomorph temperature of the virtual state point from the slope of a plot of the ensuing energy or force, respectively, compared to those of the original state. Each virtual state gives a point on the same isomorph as that on which the simulated or 'reference' state lies. The advantage of these latter two methods is that for a particular isomorph a simulation at a single density and temperature is only required, and the density 'jumps' to the virtual states can be relatively large therefore compared to the first, small step method described first.

The isomorphs of the LJ system have already been investigated extensively, $e.g.$, in Refs. [24–27]. Relatively recently it has been shown that the isomorphs for the fluid TC, when close to the freezing line, are to a very good approximation parallel to it. This means that the isomorph line can be expressed as a function of the reduced number density, $\rho/\rho_{\rm fr}(T)$, where $\rho_{\rm fr}$ is the temperature-dependent freezing density which is now known accurately for the LJ system [28, 29]. This feature is termed 'freezing density scaling', (FDS). The FDS collapse of transport coefficient values in MU is observed, perhaps surprisingly, even at low gas-like densities, (see Refs. [27, 30–33] and, from the present authors, see Ref. [17]) where the systems are not LJ isomorphs. A suggested reason for this will emerge from the discussion in this work.

The quantity $\simeq \rho_{\rm fr}^{-1/3}$ could be viewed as an effective hard sphere diameter, $\sigma_{\rm HS}$, and therefore $\rho/\rho_{\rm fr}(T)$ of the LJ system can be considered to be equivalent to the same ratio, $\rho/\rho_{\rm fr}$ for the hard sphere system (which is not temperature dependent). Hence the role of the FDS is to map the LJ system at any temperature onto its nearest equivalent hard sphere system, and hence implicitly having the same excess entropy as the HS fluid.

Comparisons between the transport coefficients of the HS and LJ system within the context of isomorphs have already been made in the literature. Nevertheless, some new aspects and insights of their relative behavior $e.g.$, in regard to FDS, are brought our here. In addition, the exercise of treating the LJ system as a pseudo $n = 12$ IP case (which form perfect isomorphs) has already been developed in the literature by Ashurst and Hoover [34], and Woodcock [35], and the present work therefore builds to a large extent on their pioneering treatments. This investigation develops these themes within the context of the relatively recently developed isomorph theory.

This work continues our previous study into the FDS of the transport coefficients in the LJ liquid and supercritical fluid parts of its phase diagram [17]. Our previous treatment on the isomorphic behavior of $\eta_{\rm s}$ and D is extended to include the thermal conductivity. Comparisons between the isomorph scaling behavior of the hard sphere and LJ systems

Tab. 1. A list of the acronyms and their definitions used in this work

Acronym	Definition
DIC	Direct isomorph check
FDS	Freezing density scaling
HS	Hard sphere
IP	Inverse power
LJ	Lennard-Jones
MD	Molecular dynamics
MU	Macroscopic unit
TC	Transport coefficient

are made, and further insights into their relative behavior are given, which is covered in the next section.

II. Theory

For the shear viscosity and thermal conductivity, the isomorph or MU scaled values are $\tilde{\eta}_{\rm s} = \eta_{\rm s}\rho^{-2/3}T^{-1/2}$ and $\tilde{\lambda} = \lambda\rho^{-2/3}T^{-1/2}$, respectively, and for the self-diffusion coefficient, $\tilde{D} = D\rho^{1/3}T^{-1/2}$. This scaling was applied to both the HS and LJ transport coefficients. The first two TC are collective properties while the third is based on a single-particle quantity, which gives rise to some qualitative differences in the appearance of the density dependence of these two classes of TC.

The Enskog theory of transport coefficients of hard spheres is the starting point of the present analysis. The HS system can be considered to be the most fundamental example of a perfect isomorph forming model system.

The HS shear viscosity, $\eta_{\rm s}$, is obtained from Eq. (18) in Ref. [36] (and below Eq. (10) in Ref. [37]) as follows,

$$\begin{aligned}\eta_{\rm s,E} &= \eta_{\rm s,0}\left[\frac{1.016}{g(\sigma)} + 0.8128b\rho + 0.7737g(\sigma)b^2\rho^2\right] = \\ &= \eta_{\rm s,0}\frac{\rho b}{Z-1}\left[1.016\left(1+\frac{2}{5}(Z-1)\right)^2 + \frac{48}{25\pi}(Z-1)^2\right], \\ \eta_{\rm s,0} &= \frac{5}{16\sigma^2}\left(\frac{mk_{\rm B}T}{\pi}\right)^{1/2}, \end{aligned} \quad (1)$$

where σ is the hard sphere diameter, $b = 2\pi\sigma^3/3$, $g(r)$ is the radial distribution function and $Z = P/\rho k_{\rm B}T$ is the compressibility factor (P is the pressure). The value of the shear viscosity in the limit of zero density from kinetic theory is, $\eta_{\rm s,0}$. It is convenient to set σ, m and $k_{\rm B}$ to unity in the following equations. Now as in MU, $\tilde{\eta}_{\rm s} = \eta_{\rm s}\rho^{-2/3}T^{-1/2}$, then

$$\begin{aligned}\tilde{\eta}_{\rm s,E} &= \tilde{\eta}_{\rm s,0}\left[\frac{1.016}{g(1^+)} + 0.8128b\rho + \ 0.7737g(1^+)b^2\rho^2\right] = \\ &= \tilde{\eta}_{\rm s,0}\frac{\rho b}{Z-1}\left[1.016\left(1+\frac{2}{5}(Z-1)\right)^2 + \frac{48}{25\pi}(Z-1)^2\right], \\ \tilde{\eta}_{\rm s,0} &= \frac{5}{16\sqrt{\pi}}\rho^{-2/3}. \end{aligned} \quad (2)$$

The radial distribution function on contact of the hard spheres tends to 1 in the zero density limit. When expressed in MU the temperature does not appear in Eq. (2). Similarly for the thermal conductivity, λ [38],

$$\begin{aligned}\tilde{\lambda}_{\rm E} &= \tilde{\lambda}_0\left[\frac{1.02522}{g(1^+)} + 1.23026b\rho + 0.776516g(1^+)b^2\rho^2\right] = \\ &= \tilde{\lambda}_0\frac{\rho b}{Z-1}\left[1.02522\left(1+\frac{3}{5}(Z-1)\right)^2 + \frac{32}{25\pi}(Z-1)^2\right], \\ \tilde{\lambda}_0 &= \frac{75}{64\sqrt{\pi}}\rho^{-2/3}. \end{aligned} \quad (3)$$

The Enskog formula for the self-diffusion coefficient, D, is [38, 39],

$$\begin{aligned}\tilde{D}_{\rm E} &= \tilde{D}_0\frac{1.01896}{g(1^+)} = 1.01896\tilde{D}_0\frac{b\rho}{Z-1}, \\ \tilde{D}_0 &= \frac{3}{8\rho\sqrt{\pi}}\rho^{1/3} = \frac{3}{8\sqrt{\pi}}\rho^{-2/3}, \end{aligned} \quad (4)$$

in MU. Eqs. (1)-(4) show that in the low density limit all three transport coefficients in MU diverge as $\sim \rho^{-2/3}$, but with no temperature dependence. An analysis in terms of the excess entropy, $s_{\rm ex}$, gives a term [40], $\sim s_{\rm ex}^{-2/3}$, because the excess entropy becomes increasingly proportional to ρ as it decreases in the low density limit. The equation of state of hard spheres, Z, used here in the Enskog formulas is the analytic expression 'mKLM' given in Eq. (4) in Ref. [41].

Khrapak and coworkers discovered freezing density scaling [27, 30–33] for LJ and the noble gas liquids. Consider a potential isomorph line which passes through the state point, T_0, ρ_0. Written formally, the freezing isomorph line (using the subscript, 'i') in the form of a temperature dependent density, $\rho_i(T)$ is shifted away from the freezing density line by a constant ratio. This is specified as follows,

$$R = \rho_0/\rho_{\rm fr}(T_0), \quad \rho_i(T) = R\rho_{\rm fr}(T), \quad (5)$$

which may be said to be 'parallel' to the freezing line, where the density shift factor, R is the ratio of the reference density, ρ_0, divided by the density along the freezing line, both when $T = T_0$. For the HS system, $\rho_i(T)$ is a vertical line when T is along the ordinate axis.

The properties of the HS system and its TC have been used in previous studies to explain the trends in polyatomic real molecules, some of which might be considered to be far removed from the LJ model system ($e.g.$, hexadecane). For example Dymond and coworkers used a e analogy [8], in a series of publications and found that the transport coefficients, 'X', of a wide range of compounds determined by experiment shared a common relationship [8, 42, 43], of the form, $\tilde{X} = F_X(\rho/\rho_{\rm D,0})$, where $\rho_{\rm D,0}$ is a temperature-dependent reference density in the high pressure limit, which is the same for all of the transport coefficients considered in that work. This density takes on a similar role to the freezing density in the FDS approach.

The HS and LJ TC data were fitted to the function in this work with,

$$\tilde{X} = a_X x^{-2/3} + b_X x + c_X x^2 + d_X x^3 + e_X e^{f_x x}, \quad (6)$$

where $x \equiv \rho/\rho_{\rm fr}(T)$, and $\rho_{\rm fr}$, is calculated from the Schultz and Kofke formula given in Refs. [28, 29]. The expression in Eq. (6) bears some similarity with the Enskog formulas above for the shear viscosity and thermal conductivity, but with the extra terms is sufficiently flexible to represent accurately any departures from Enskog (even for HS) exhibited by the actual behavior of the model monatomic fluid system, which can be determined accurately by molecular dynamics simulations. Eq. (6) can also be used to represent the self-diffusion coefficient data, with some parameters having different signs from those of the shear viscosity and thermal conductivity cases. Tab. 2 gives the values of the constants

in Eq. (6) for each transport coefficient for the HS and LJ systems.

The curves for each transport coefficient given by the expression in Eq. (6) fitted to the LJ MD simulation data can be used to express the TC in various units for an arbitrary state point in the LJ fluid phase diagram. First, for any given (ρ, T) state point, that equation gives the transport coefficient in MU units, after first determining the dimensionless density ('x' in the equation) at that temperature. Hence the transport coefficients at that state point can be computed in LJ units of ϵ, σ and the mass of the particle from their definitions, *i.e.*, $\eta_s = \tilde{\eta}_s \rho^{2/3} T^{1/2}$, and $\lambda = \tilde{\lambda} \rho^{2/3} T^{1/2}$ and $D = \tilde{D} \rho^{-1/3} T^{1/2}$. Following on from this step, these transport coefficients in LJ units can be converted to SI units for any given small molecule which can be represented by a LJ potential to a reasonable approximation, using its value of ϵ and σ.

III. Results

This section focusses on comparing the behavior of the HS and LJ TC when the TC are expressed in terms of MU and the density is normalized by the freezing density in both cases. First the TC behavior of hard sphere fluids is considered.

III. 1. Hard Spheres

Fig. 1 shows the three transport coefficients of hard spheres in isomorph units plotted as a function of $\rho/\rho_{\rm fr}$.

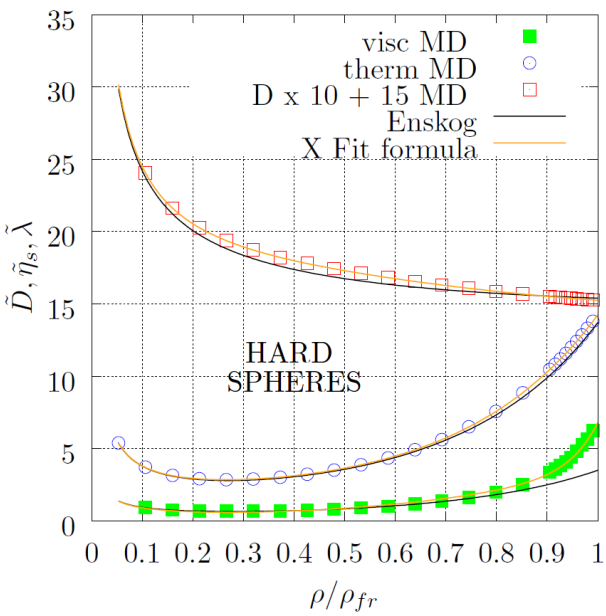

Fig. 1. Hard sphere transport coefficient data taken from Refs. [41, 44] and scaled to be in isomorph units are shown by symbols. Fits to these data using the generic formula in Eq. (6) are shown as continuous red lines on the figure. The least squares fit parameters for each transport coefficient are given in Tab. 2. The diffusion coefficient data are shifted upwards by 15 and multiplied by $\times 10$ for clarity. The Enskog formula predictions using Eqs. (1)–(4) are also shown as black continuous lines on the figure. All quantities are normalized to make them dimensionless

For hard spheres [41], $\rho_{\rm fr} = 0.9392(1)$ and is temperature independent. The data is taken from Refs. [41, 44]. The expression given in Eq. (6) fitted to these data are also given in Fig. 1. The fit parameters for the expression in Eq. (6) are presented in Tab. 2. The predictions using the Enskog formulas given in Eqs. (1)–(4) are also shown on the figure. The Enskog expressions agree well with the MD data up to $\rho \sim 0.8$ for the viscosity and practically up to freezing for the thermal conductivity. The Enskog formula for $\tilde{D}$ underestimates the MD values for intermediate densities as is well known and due to a 'microhydrodynamic' process discussed in Ref. [41]. The Enskog formula for $\tilde{D}$ overestimates the simulation values at high density close to the freezing point.

Tab. 2. The parameters for the formula given in the Eq. (6) obtained from a least squares fit to the MD simulation data. The fit parameters for the hard sphere ('HS') and Lennard-Jones potential ('LJ') systems are given for each transport coefficient

	HS $\tilde{D}$	HS $\tilde{\eta}_s$	HS $\tilde{\lambda}$
a_X	0.238321	0.184296	0.703623
b_X	0.332723	1.647983	2.150955
c_X	−0.653124	−5.180327	−1.059641
d_X	0.302959	7.4909157	1.288698
e_X	−0.183643	2.593997×10^{-9}	0.214774
f_X	0.0667652	20.747125	3.950194
	LJ $\tilde{D}$	LJ $\tilde{\eta}_s$	LJ $\tilde{\lambda}$
a_X	0.204316	0.13240	0.284728
b_X	0.340595	1.34699	−2.98120
c_X	−0.826568	−2.35086	4.95168
d_X	0.455079	3.352267	4.14386
e_X	−0.114637	2.286456×10^{-4}	2.13376
f_X	0.188901	9.305488	0.52122

Tab. 3. Parameters relating to the minimum and freezing point of $\tilde{\eta}_s$ and $\tilde{\lambda}$ for the hard sphere ('HS') and Lennard-Jones potential ('LJ') systems. The quantity, $x_{\rm m}$, is the value of $\rho/\rho_{\rm fr}$ at the minimum value of the quantity in the line above. $\tilde{X}_{\rm fr}$ is the value of the transport coefficient 'X' at the freezing point in MU from the generic expression in Eq. (6)

	HS	LJ
$\tilde{\eta}_{\rm m,s}$	0.634	0.578
$x_{\rm m}$	0.342	0.260
$\tilde{\lambda}_{\rm m}$	2.77	2.75
$x_{\rm m}$	0.263	0.265
$\tilde{\eta}_{\rm fr,s}$	6.80	5.00
$\tilde{\lambda}_{\rm fr}$	14.2	9.90
$\tilde{D}_{\rm fr}$	0.0246	0.0350

Tab. 3 gives a list of some key quantities that were derived from Fig. 1. There is a minimum in $\tilde{\eta}_s$ which has a value of 0.634 at $\rho/\rho_{fr} = 0.342$, and these values for $\tilde{\lambda}$ are 2.837 and 0.265, respectively. There is no minimum (nor maximum) in $\tilde{D}$, η_s, λ and D. The values of the hard sphere, $\tilde{\eta}_s$, $\tilde{\lambda}$ and $\tilde{D}$ at the freezing density using the fit formula in Eq. (6) are, 6.80, 14.2 and 0.0246, respectively.

Now we compare how the LJ model system transport coefficients compares with the HS fluid.

III. 2. Lennard-Jones

The extent to which the expressions given in Eq. (6) reproduce the LJ simulation data for the transport coefficients is investigated. The MD data for LJ η_s and D were taken from the work of Meier [45]. The state points used are indicated in Fig. 2, with each symbol on the figure indicates a state point where a MD simulation of the TC was carried out.

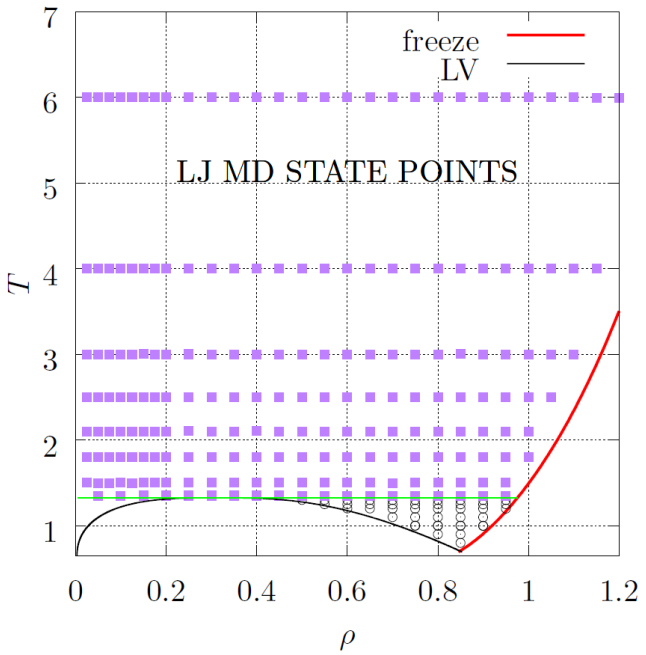

Fig. 2. The LJ state points on its phase diagram at which the η_s and D MD simulation calculations were carried out. These data are taken from Ref. [45]. The liquid-vapor binodal curve ('LV') and freezing line ('freeze') are shown

III. 3. Shear Viscosity

Fig. 3 shows the LJ shear viscosity as a function of density along several isotherms, where both quantities are given in LJ units. These data cover both the liquid and supercritical fluid regions, encompassing the temperature interval, $0.7 \leq T \leq 6.0$. The LJ MD shear viscosity data extends from quite low densities where the systems exhibit gas-like behavior to high liquid-like densities close to the freezing line. The global expression for $\tilde{\eta}_s$ given in Eq. (6) was fitted to all of the data in that figure. When converted back to LJ units for each state point the expression is seen in Fig. 3 to

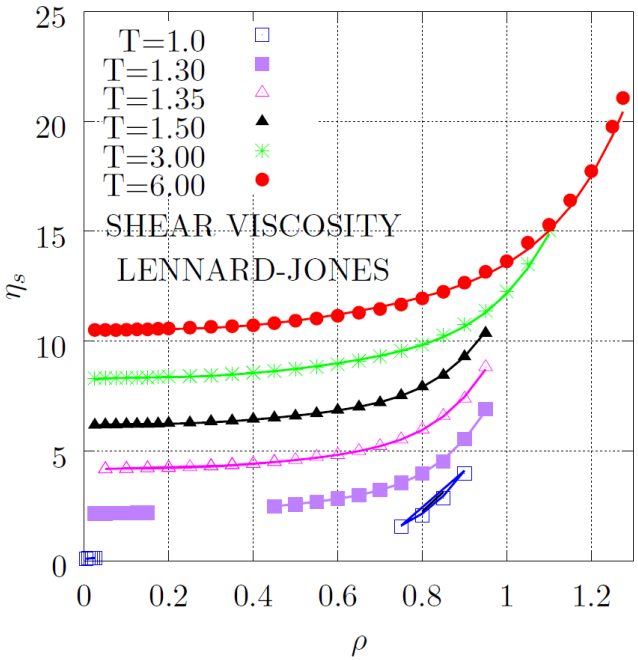

Fig. 3. The shear viscosity, η_s, as a function of ρ for the LJ fluid in the liquid and supercritical fluid states [45]. The continuous lines are by least squares fitting the entire data on the figure to the expression given in Eq. (6)

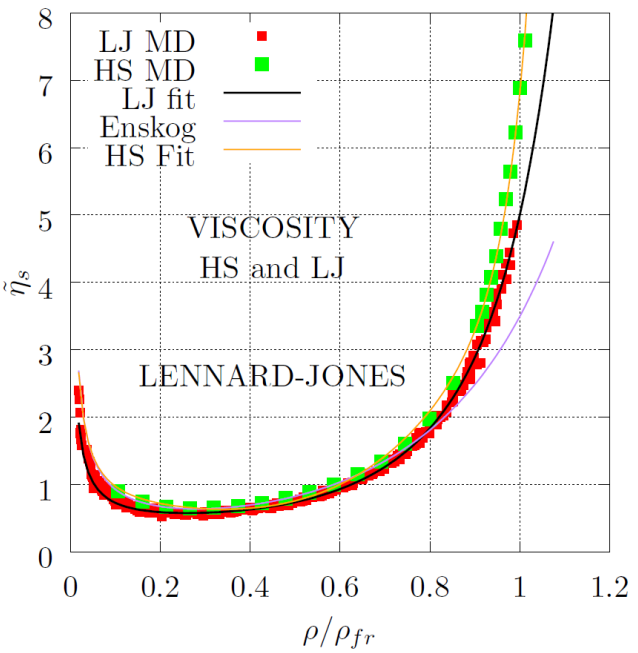

Fig. 4. As for Fig. 3 except that the MD LJ η_s values ('LJ MD') are scaled in macroscopic units and the density is scaled by the freezing density for each case. The continuous lines are using given by least squares fitting the whole HS ('HS fit') and LJ ('LJ fit') data on the figure to the expression given in Eq. (6). The Enskog HS η_s formula ('Enskog' on the figure) from Eq. (2) is also shown. The HS MD data ('HS MD') are also presented [41]

reproduce the MD viscosity values well for each isotherm, even at temperatures in the liquid part of the LJ phase diagram (note that the expression in Eq. (6) is fitted on the assumption that the whole fluid phase TC are on isodynes). The agreement at low densities is particularly noteworthy because these state points are not in the isomorph region for thermodynamic properties of the LJ phase diagram ($i.e.$, at densities less than about the critical point value of 0.316). In that region the Pearson correlation coefficient between the potential energy and the virial is much smaller than *ca.* ~ 0.9, which means that it is not an isomorph at sub-critical point densities [24–26].

Fig. 4 shows the same LJ quantities expressed in MU as a function of density, applying the FDS normalization. The whole data set is plotted. The corresponding data for the HS system is also given. The agreement between the HS and LJ data is generally good, both showing a minimum in $\tilde{\eta}_s$ separated by two ascending regions, in the gas-like regime of the left and in the liquid-like extreme on the right. Differences are apparent for *ca.* $\rho/\rho_{fr} > 0.9$ however, where the HS normalized viscosities increase more rapidly than that of the LJ. This is intuitively understandable, as near the freezing point a LJ assembly of particles is able to arrange and evolve with time cooperatively, because of the range of the potential compared to the particle's diameter. In contrast the hard sphere potential is short ranged and a delta function at $r = \sigma$ (and in fact this distance defines its diameter) which will make the HS system more prone to forming transient 'jammed' arrangements. This feature cannot be eliminated by 'scaling' in any obvious or physically meaningful way as this difference in behavior is a direct consequence of the difference in the shapes of the two pair potentials.

III. 4. Self-Diffusion Coefficient

Fig. 5 presents the self-diffusion coefficient values as a function of density, both in LJ units, for several isotherms in the liquid and supercritical region. The same good reproduction as for the shear viscosity of the MD data with the global fit function of Eq. (6) (when the MU scaled TC predicted at each state point are converted back to LJ units) is evident. Fig. 6 shows the same data plotted in MU units, combined with the same quantities for the hard sphere system. Again as for $\tilde{\eta}_s$, the HS and LJ sets of $\tilde{D}$ data when expressed in this normalized format agree very closely across the fluid range.

III. 5. Thermal Conductivity

Thermal conductivity MD data for the LJ system is not as extensively available as for η_s and D, and λ values from a number of literature sources were gathered for the present analysis. These λ data in MU units are plotted as a function of the freezing density scaled density in Fig. 7. The different sources of $\tilde{\lambda}$ are distinguished on the figure. Fig. 8 shows the same data plotted in MU units as a function of ρ/ρ_{fr}, compared with the corresponding HS data. Bearing in mind the relatively limited number of data points at low density (compared to the equivalent plots for η_s and D), and the somewhat larger scatter (particularly in the vicinity of the critical point) the agreement between the key features of the HS and

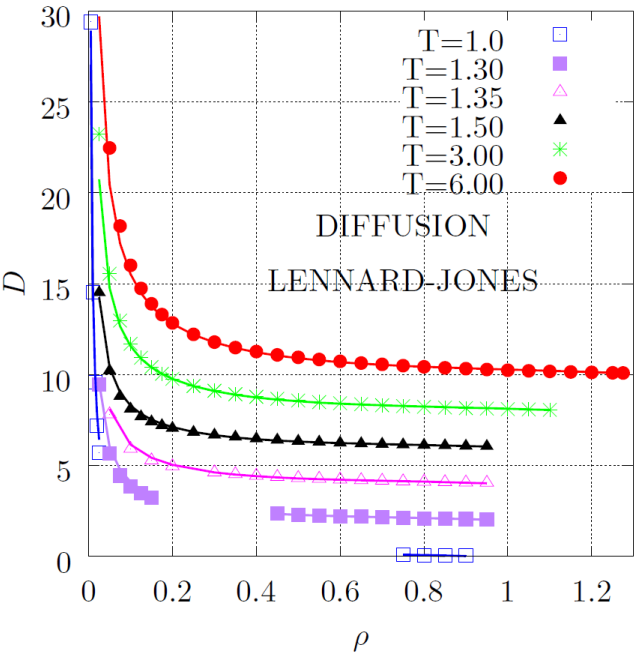

Fig. 5. As for Fig. 3 except the self-diffusion coefficient, D, values as a function of ρ along several LJ liquid and supercritical fluid states are shown [45]. The continuous lines on the figure are least squares fits to the MD data shown on the figure using the formula in Eq. (6)

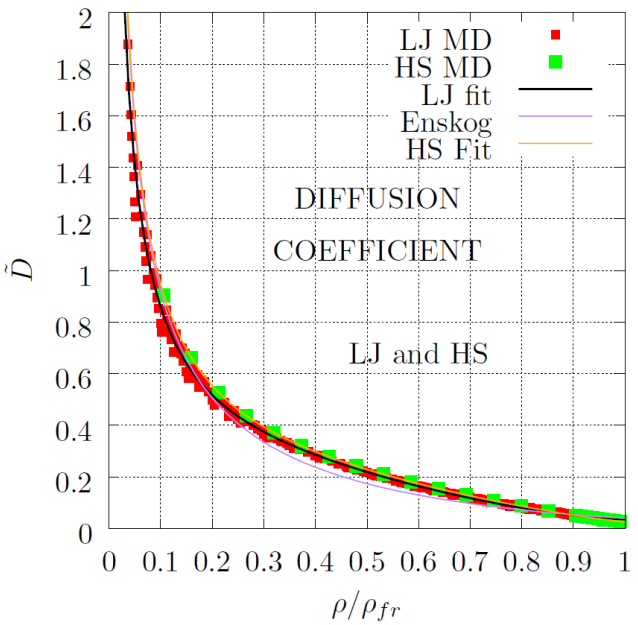

Fig. 6. As for Fig. 4 except that the MD LJ $\tilde{D}$ values ('LJ MD') are scaled in macroscopic units and the density is scaled by the freezing density for each case. The continuous lines are using given by least squares fitting the entire HS ('HS fit') and LJ ('LJ fit') data on the figure to the expression given in Eq. (6). The HS MD values ('HS MD') are presented [41]. The Enskog formula for the D ('Enskog') from Eq. (4) are shown

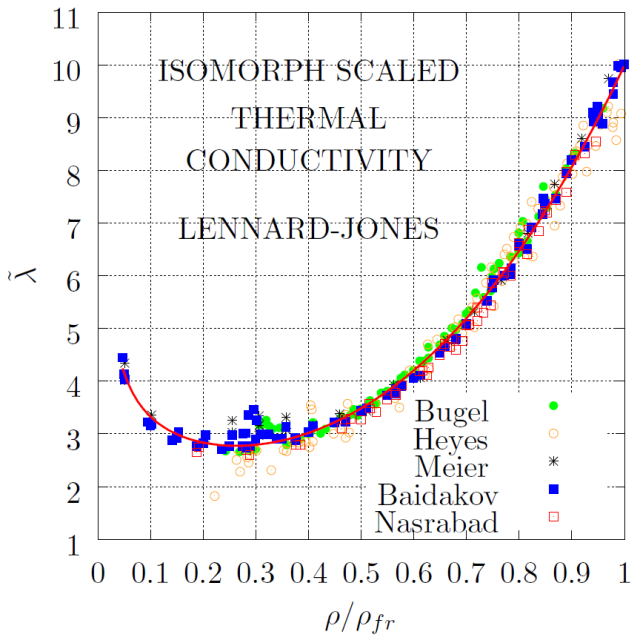

Fig. 7. The reduced thermal conductivity, $\tilde{\lambda}$, as a function of $\rho/\rho_{\rm fr}$ for the LJ fluid in the liquid and supercritical fluid from various publications. The solid lines are obtained by least squares fitting the whole MD data on the figure to the formulas presented in Eq. (6). This is the solid red line on the figure. Key for the sources of λ : Ref. [46] ('Bugel'), Ref. [47] ('Heyes'), Ref. [45] ('Meier'), Ref. [48] ('Baidakov') and Ref. [49] ('Nasrabad')

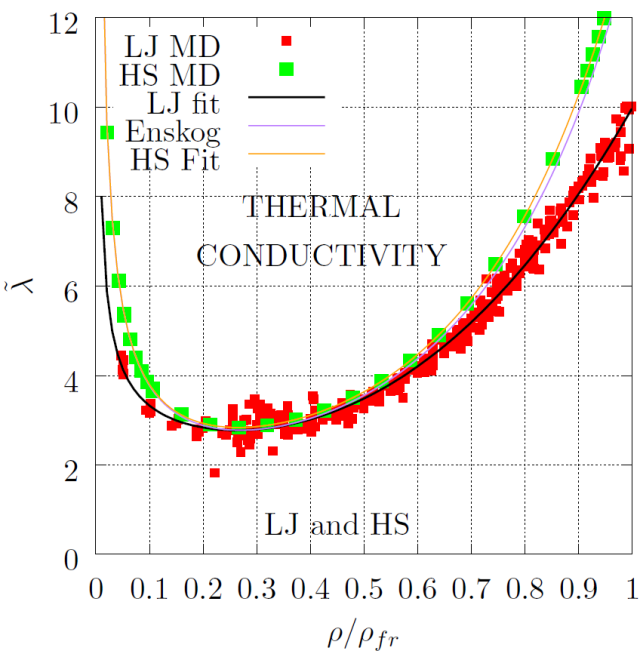

Fig. 8. As for Fig. 4 except that the MD LJ $\tilde{\lambda}$ values ('LJ MD') as a function of $\rho/\rho_{\rm fr}$ are compared with the same quantities from the HS fluid. The continuous lines are obtained by least squares fitting the entire HS ('HS fit') and LJ ('LJ fit') data on the figure to the expression given in Eq. (6). The Enskog HS $\eta_{\rm s}$ formula ('Enskog' on the figure) from Eq. (3) is also shown. The HS MD data ('HS MD') are also presented [44]

LJ systems is again generally quite good, as for the other two transport coefficients. In the region of the critical point there is enhancement of the thermal conductivity [45], which explains the large fluctuations in the scaled thermal conductivity in the vicinity of $\rho/\rho_{\rm fr} \simeq 0.32$. Just as for the corresponding figure for the shear viscosity, the HS data rise more rapidly that those from the LJ potential close to freezing, indicating again that the assembly of particles formed by the HS system is more 'constrained' dynamically near the freezing density. The fit expression in Eq. (6) does not agree well with the HS MD data and the Enskog formula in Eq. (3) in the low density region because of the limited number of MD data points there.

Tab. 3 also presents a summary of the scaled parameters for the minima and freezing point parameters of the LJ system. The minimum value of the viscosity, $\tilde{\eta}_{\rm m,s}$, and thermal conductivity, $\tilde{\lambda}_{\rm m}$, are quite similar for the hard sphere and LJ systems. The densities at which their corresponding reduced densities reach a minimum, $x_{\rm m}$, are slightly more different as the curves are quite flat in the region of the minimum, which makes its determination more sensitive to the statistical uncertainties in the fits to the MD data. Also in this intermediate density region it might be expected that the differences in the shapes of the two potentials to have an effect on precisely where the transition from gas-like to liquid-like behavior takes place (as represented by the value of $x_{\rm m}$).

Tab. 3 also shows that at the freezing point, ($i.e.$, where, $x = \rho/\rho_{\rm fr} = 1$), these quantities are about $\sim$ 30% smaller for the LJ system. In contrast, the self-diffusion constants, $\tilde{D}$ is about $\sim$ 40% larger for the LJ system. The trends in these quantities are intuitively reasonable and self-consistent, and as noted above, it might be expected that the LJ system is more 'fluid-like' at the freezing point than the hard sphere system because of the comparitively long range nature of the LJ potential which might facilitate the collective motion of the particles compared to the HS system.

Khrapak and Khrapak also analysed the shear viscosity and thermal conductivity of LJ, hard spheres and liquified noble gases along certain isotherms [30–32]. The values for the minima and freezing point in Tab. 3 are close to those given in Ref. [33].

For the much studied LJ state point, $\rho = 0.8442$ and $T = 0.722$ (where $\rho_{\rm fr} = 0.854$) the shear viscosity and self-diffusion coefficients in LJ units are from fit formulas, $3.5(2)$ and $0.0326(1)$, using the generic expression given in Eq. (6), which are at worst within 8% and 1% of the literature values [13, 14, 35]. This is a very demanding test of the fit formula as this state point is close to the triple point, deep in the liquid region where the attractive part of the LJ potential is most influential.

IV. Conclusions

By plotting the transport coefficients in macroscopic units against the density scaled by the freezing density, so-called freezing density scaling, which is a novel aspect of this work compared to previous literature, it has been possible to make a more informative comparison between the

behavior of the hard sphere and Lennard-Jones systems, and come to more definitive conclusions.

Further analysis carried out in this study leads to conclusions about the possible origin of the common occurrence of isodynes over the whole of the fluid phase diagram in this work. The LJ transport coefficients do exhibit an isomorph unit collapse at low densities, but corresponding to that of *another* model system, which is represented well by hard spheres. This is because the transport coefficients are more sensitive to the repulsive part of the potential than other properties, *especially* at low densities. The insensitivity at gas-like and intermediate densities is also because another characteristic lengthscale becomes important for the system, not just the particle diameter (which dominates at liquid-like densities). The mean distance between collisions, l, which is important in determining the transport coefficients at low density, diverges in the low density range. The distance, l, is an important parameter in determining the TC of gas-like systems, and as density decreases l becomes greater than the particle diameter and less sensitive to the details of the interaction between the particles (beyond the minimum in the LJ potential in the LJ case) [40].

As is well known, the hard sphere system, like the inverse power potential system, exhibits isomorphs at all densities which makes these simple potentials useful reference systems for the transport coefficients of the LJ fluid across its phase diagram. The present investigation quantifies these parallels in more detail, and gives further insights into the origins of these relationships between the behavior of these closely related potential systems.

Acknowledgment

DMH would like to thank Dr. T. Crane (Department of Physics, Royal Holloway, University of London, UK) for helpful software support.

References

[1] B.L. Holian, *Modeling shock-wave deformation via molecular dynamics*, Phys. Rev. A **37**, 2562–2568 (1988).

[2] F.J. Uribe, W.G. Hoover, C.G. Hoover, *Maxwell and Cattaneo's Time-Delay Ideas Applied to Shockwaves and the Rayleigh-Bénard Problem*, Comp. Meth. Sci. Technol. **19**, 5–12 (2013).

[3] M.K. Poshtegal, S.A. Mirbagheri, *Simulation and modelling of heavy metals and water quality parameters in the river*, Scient. Rep. **13**, 3020 (2023).

[4] J.-P. Hansen, I.R. McDonald, *Theory of Simple Liquids*, 4^{th} ed., Academic Press, Amsterdam (2013).

[5] S.K. Loyalka, E.L. Tipton, R.V. Tompson, *Chapman-Enskog solutions to arbitrary order in Sonine polynomials I: Simple, rigid-sphere gas*, Physica A **379**, 417–435 (2007).

[6] J.R. Dorfman, H. van Beijeren, T.R. Kirkpatrick, *Contemporary Kinetic Theory of Matter*, Cambridge University Press, Cambridge (2021).

[7] S. Chapman, T.G. Cowling, *The Mathematical Theory of Non-Uniform Gases*, Cambridge University Press, Cambridge (1991)

[8] J.H. Dymond, *Corrected Enskog theory and the transport coefficients of liquids*, J. Chem. Phys. **60**, 969–973 (1974).

[9] J.W. Dufty, *Shear stress correlations in hard and soft sphere fluids*, Molec. Phys. **100**, 2331–2336 (2002).

[10] J.W. Dufty, M.H. Ernst, *Exact short time dynamics for steeply repulsive potentials*, Molec. Phys. **102**, 2123–2135 (2004)

[11] J.W. Dufty, *Stress tensor and elastic properties for hard and soft spheres*, Gran. Matt. **14**, 271–275 (2012).

[12] W.G. Hoover, M. Ross, K.W. Johnson, D. Henderson J.A. Barker, B.C. Brown, *Soft-Sphere Equation of State*, J. Chem. Phys. **52**, 4931 (1970).

[13] D.M. Heyes, D. Dini, L. Costigliola, J.C. Dyre, *Transport coefficients of the Lennard-Jones fluid close to the freezing line*, J. Chem. Phys. **151**, 204502 (2019).

[14] D.M. Heyes, D. Dini, E.R. Smith, *Single trajectory transport coefficients and the energy landscape by molecular dynamics simulations*, J. Chem. Phys. **152**, 194504 (2020).

[15] W.G. Hoover, A.J.C. Ladd, R.B. Hickman, B.L. Holian, *Bulk viscosity via nonequilibrium and equilibrium molecular dynamics*, Phys. Rev. A **21**, 1756–1760 (1980).

[16] D.M. Heyes, S. Pieprzyk, A.C. Brańka, *Bulk viscosity of hard sphere fluids by equilibrium and nonequilibrium molecular dynamics simulations*, J. Chem. Phys. **157**, 114502 (2022).

[17] D.M. Heyes, D. Dini, S. Pieprzyk, A.C. Brańka, *Departures from perfect isomorph behavior in Lennard-Jones fluids and solids*, J. Chem. Phys. **158**, 134502 (2023).

[18] N. Gnan, T.B. Schrøder, U.R. Pedersen, N.P. Bailey, J.C. Dyre, *Pressure-energy correlations in liquids. IV. "Isomorphs" in liquid phase diagrams*, J. Chem. Phys. **131**, 234504 (2009).

[19] T.B. Schrøder, N. Gnan, N.P. Bailey, U.R. Pedersen, J.C. Dyre, *Pressure-energy correlations in liquids. V. Isomorphs in generalized Lennard-Jones systems*, J. Chem. Phys. **134**, 164505 (2011).

[20] T.S. Ingebrigtsen, T.B. Schrøder, J.C. Dyre, *Isomorphs in Model Molecular Liquids*, J. Phys. Chem. B **116**, 1018–1034 (2012).

[21] J.C. Dyre, *Hidden Scale Invariance in Condensed Matter*, J. Phys. Chem. B **118**, 10007–10024 (2014).

[22] Z. Sheydaafar, *Isomorphs and pseudoisomophs in molecular liquid models*, PhD thesis, Roskilde University, Denmark (2021).

[23] K. Moch, N.P. Bailey, *Isomorph invariant dynamic mechanical analysis: A molecular dynamics study*, Phys. Rev. Mat. **6**, 085602 (2022).

[24] T.S. Ingebrigtsen, L. Bøhling, T.B. Schrøder, *Thermodynamics of condensed matter with strong pressure energy correlations*, J. Chem. Phys. **136**, 061102 (2012).

[25] L. Bøhling, T.S. Ingebrigtsen, A. Grzybowski, M. Paluch, J.C. Dyre, T. B. Schrøder, *Scaling of viscous dynamics in simple liquids: theory, simulation and experiment*, New J. Phys. **14**, 113035 (2012).

[26] N.P. Bailey, T.B. Schrøder, J.C. Dyre, *Variation of the dynamic susceptibility along an isochrone*, J. Chem. Phys. **90**, 042310 (2014).

[27] S.A. Khrapak, *Gas-liquid crossover in the Lennard-Jones system*, J. Chem. Phys. **156**, 116101 (2022).

[28] A.J. Schultz, D.A. Kofke, *Comprehensive high-precision high-accuracy equation of state and coexistence properties for classical Lennard-Jones crystals and low-temperature fluid phases*, J. Chem. Phys. **149**, 204508 (2018).

[29] A.J. Schultz, D.A. Kofke, *Erratum: 'Comprehensive high-precision high-accuracy equation of state and coexistence properties for classical Lennard-Jones crystals and low temperature fluid phases'*, J. Chem. Phys. **153**, 059901 (2020).

[30] S.A. Khrapak, A.G. Khrapak, *Transport properties of Lennard-Jones fluids: Freezing density scaling along isotherms*, Phys. Rev. E **103**, 042122 (2021).

[31] S.A. Khrapak, A.G. Khrapak, *Freezing Temperature and Density Scaling of Transport Coefficients*, J. Phys. Chem. Lett. **13**, 2674–2678 (2022).
[32] S.A. Khrapak, A.G. Khrapak, *Freezing density scaling of fluid transport properties: Application to liquefied noble gases*, J. Chem. Phys. **157**, 014501 (2022).
[33] S.A. Khrapak, A.G. Khrapak, *Minima of shear viscosity and thermal conductivity coefficients of classical fluids*, Phys. Fluids **34**, 027102 (2022).
[34] W.T. Ashurst, W.G. Hoover, *Dense fluid shear viscosity and thermal conductivity—the excess*, AIChE Journal **21**, 410–411 (1975).
[35] L.V. Woodcock, *Equation of State for the Viscosity of Lennard-Jones Fluids*, AIChE Journal **52**, 438–446 (2006).
[36] J.J. Erpenbeck, W.W. Wood, *Self-diffusion coefficient for the hard-sphere fluid*, Phys. Rev. A **43**, 4254–4261 (1991).
[37] J.J. Erpenbeck, W.W. Wood, *Molecular Dynamics Calculations of Shear Viscosity Time-Correlation Functions for Hard Spheres*, J. Stat. Phys. **24**, 455–468 (1981).
[38] P. Résibois, M. de Leener, *Classical Kinetic Theory of Fluids*, p. 168, John Wiley & Sons, New York (1977).
[39] J.J. Erpenbeck, W.W. Wood, *Molecular-dynamics calculations of the velocity autocorrelation function: Hard-sphere results*, Phys. Rev. A **32**, 412–422 (1985).
[40] I.H. Bell, R. Messerly, M. Thol, L. Costigliola, J.C. Dyre, *Modified Entropy Scaling of the Transport Properties of the Lennard-Jones Fluid*, J. Phys. Chem. B **123**, 6345–6363 (2019).
[41] S. Pieprzyk, A.C. Brańka, M.N. Bannerman, M. Chudak, D.M. Heyes, *Thermodynamic and dynamical properties of the hard sphere system revisited by molecular dynamics simulation*, Phys. Chem. Chem. Phys. **21**, 6886 (2019).
[42] J.H. Dymond, *A Theory-Based Method for Correlation and Prediction of Dense-Fluid Transport Properties*, Int. J. Thermophys. **18**, 303–312 (1997).
[43] J.H. Dymond, M.J. Assael, [In:] *Transport Properties of Fluids: Their correlation, prediction and estimation*, Eds. J. Millat, J.H. Dymond, C.A. Nieto de Castro, Chap. 10, p. 226, Cambridge University Press, New York (1996).
[44] S. Pieprzyk, A.C. Brańka, D.M. Heyes, M.N. Bannerman, *A comprehensive study of the thermal conductivity of the hard sphere fluid and solid by molecular dynamics simulation*, Phys. Chem. Chem. Phys. **22**, 8834–8845 (2020).
[45] K. Meier, *Computer Simulation and Interpretation of the Transport Coefficients of the Lennard-Jones Model Fluid*, PhD thesis, University of the Federal Armed Forces Hamburg (2002).
[46] M. Bugel, G. Galliero, *Thermal conductivity of the Lennard-Jones fluid: an empirical correlation*, Chem. Phys. **352**, 249–257 (2008).
[47] D.M. Heyes, *Transport coefficients of Lennard-Jones fluids: A molecular-dynamics and effective-hard-sphere treatment*, Phys. Rev. B **37**, 5677–5696 (1988).
[48] V.G. Baidakov, S.P. Protsenko, *Metastable Lennard-Jones fluids. II. Thermal conductivity*, J. Chem. Phys. **140**, 214506 (2014).
[49] A.E. Nasrabad, R. Laghaei, B.C. Eu, *Molecular theory of thermal conductivity of the Lennard-Jones fluid*, J. Chem. Phys. **124**, 084506 (2006).

David M. Heyes [PhD, University of Manchester, UK, 1977] has held postdoctoral research positions in the Vitreous State Laboratory, Department of Physics, Catholic University of America, Washington DC, USA, Department of Physical Chemistry at the University of Amsterdam, and at the Department of Chemistry, Royal Holloway, University of London. He was a Royal Society (London) 1983 University Research Fellow between 1983 and 1992, first at Royal Holloway. He is in the Department of Physics, Royal Holloway, University of London, and is a Principal Research Fellow in the Department of Mechanical Engineering, Imperial College London. His current research interests are in the area of the isomorph states of liquids and solids using statistical mechanics theory and molecular simulation, especially where applied to transport coefficients.

Sławomir Pieprzyk is assistant professor at IFMPAN, and studied technical physics at Poznań University of Technology and obtained his PhD in the Institute of Molecular Physics Polish Academy of Sciences in 2015. His research interests involve computer simulation methods and object-oriented programming, especially for simple liquids and soft matter.

Arkadiusz C. Brańka is professor at IFMPAN, and studied physics at the Adam Mickiewicz University in Poznań. He obtained his PhD in ISAS in Trieste in 1986. After his PhD he joined the Institute of Molecular Physics Polish Academy of Science, where in 2002 he received habilitation. His research interests are in the fields of structural, thermodynamics and transport properties of liquids and suspensions, liquid crystals, anomalous elasticity and simulation methods applied to particle systems.

DOI:10.12921/cmst.2023.0000026